JOURNAL OF CATALYSIS **171,** 255–267 (1997)
ARTICLE NO. CA971805

Thiophene Hydrodesulfurization over Alumina-Supported Molybdenum Carbide and Nitride Catalysts: Effect of Mo Loading and Phase

Keith R. McCrea, John W. Logan, Teresa L. Tarbuck, Jeffrey L. Heiser, and Mark E. Bussell[1]

Department of Chemistry, M.S.-9150, Western Washington University, Bellingham, Washington 98225

Received April 11, 1997; revised June 27, 1997; accepted June 28, 1997

Alumina-supported β-Mo_2C, α-$MoC_{(1-x)}$ ($x \approx 0.5$) and γ-Mo_2N catalysts with Mo loadings in the range 1.5–20 wt% have been synthesized and characterized by X-ray diffraction and pulsed chemisorption (CO and O_2) measurements. Thiophene hydrodesulfurization (HDS) activities were measured for the alumina-supported Mo carbide and nitride catalysts as well as sulfided Mo/Al_2O_3 catalysts with the same Mo loadings. The HDS activities of the catalysts after 24 h at 693 K were observed to increase according to the trend: sulfided Mo $\approx$ α-$MoC_{(1-x)}$ $<$ γ-Mo_2N $<$ β-Mo_2C. The HDS activities of the different catalysts were found to correlate in a linear fashion with their CO and O_2 chemisorption capacities for the wide range of Mo loadings investigated. Thiophene HDS turnover frequencies for the Mo carbide, nitride, and sulfided Mo catalysts are nearly identical, providing further evidence that the higher HDS activity of alumina-supported β-Mo_2C and γ-Mo_2N catalysts stems from a higher density of active sites.

INTRODUCTION

A number of investigations have been published in the literature which suggest that molybdenum carbide and nitride catalysts have strong potential for use in both the hydrodenitrogenation (HDN) (1–8) and hydrodesulfurization (HDS) (2, 3, 6, 9–13) processes. The majority of these studies have found bulk and supported Mo carbide and nitride catalysts to have HDN and HDS activities similar to or higher than those of conventional sulfide catalysts. In most cases, however, direct comparisons of catalyst activities for carbide, nitride, and sulfide catalysts have not been made as different probe molecules and experimental conditions have typically been employed to estimate the number of active sites on sulfide catalysts than are used on carbide and nitride catalysts. Specifically, room temperature CO chemisorption is most often used to measure the number of active sites on Mo carbide and nitride catalysts (14, 15) while oxygen chemisorption (temperatures vary) is used for sulfide catalysts (16–18).

A recent study in our laboratory showed alumina-supported β-Mo_2C and γ-Mo_2N catalysts (10 wt% Mo loading) to have significantly higher thiophene HDS activities (per mol Mo) than a sulfided Mo catalyst with the same Mo loading (12). However, when the catalyst activities were normalized with either their CO or O_2 chemisorption capacities, the resulting turnover frequencies were quite similar. To understand these results, characterization studies were undertaken to investigate the catalyst surfaces under reaction conditions. While thermodynamic calculations by Levy (19) suggest that molybdenum carbide and nitride should convert to molybdenum disulfide in the sulfiding conditions of an HDS reactor, X-ray diffraction analysis of fresh and tested Mo carbide and nitride catalysts showed the bulk structure of the Mo containing phase to be retained. Infrared (IR) spectroscopy of adsorbed CO on Mo carbide and nitride catalysts, however, indicated that the surfaces of the supported β-Mo_2C and γ-Mo_2N particles become sulfided under conditions similar to those present in an HDS reactor. When sulfided, adsorption sites on the Mo carbide and nitride catalysts consist of *cus* Mo^{2+} sites identical to those present on the surface of sulfided Mo catalysts. Based upon the X-ray diffraction and IR spectroscopy results, the following model (Fig. 1) was proposed for the active surface of alumina-supported Mo carbide and nitride catalysts in an HDS reactor (12).

In keeping with this model, the active sites for thiophene HDS are identical on alumina-supported Mo carbide, nitride, and sulfided Mo catalysts and, therefore, the turnover frequencies for the three catalysts are expected to be similar. While our recently published results for catalysts with a 10 wt% Mo loading provided preliminary evidence in support of this model, the current study provides data for catalysts with a more extensive range of Mo loadings (1.5–20 wt%). In addition, the HDS catalytic properties of two phases of molybdenum carbide (β-Mo_2C and α-$MoC_{(1-x)}$ ($x \approx 0.5$)) have been investigated in order to determine the effect of the Mo carbide phase on HDS activity.

[1] To whom correspondence should be addressed. E-mail: bussell@chem.wwu.edu.

0021-9517/97 $25.00

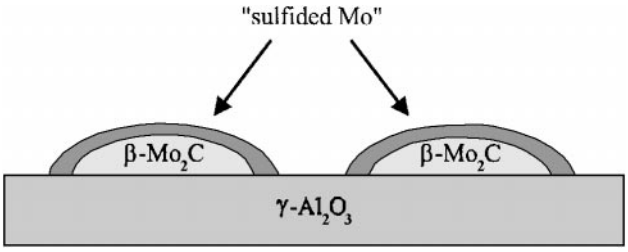

FIG. 1. Schematic representation of a Mo_2C/Al_2O_3 catalyst during thiophene HDS. Similar structures are proposed for $MoC_{(1-x)}/Al_2O_3$ and Mo_2N/Al_2O_3 catalysts.

EXPERIMENTAL SECTION

Catalyst Preparation

Alumina-supported molybdenum trioxide (MoO_3/Al_2O_3) catalysts were prepared by impregnation of γ-Al_2O_3 (Engelhard AL-3945) with aqueous solutions of ammonium heptamolybdate (J. T. Baker Co.); catalysts with Mo loadings in the range 1.5–20 wt% were prepared. For catalysts with Mo loadings greater than 13 wt%, multiple impregnations were necessary to achieve the desired Mo loading. The γ-Al_2O_3 had a BET surface area of 255 m^2/g and a pore volume of 0.60 mL/g. The alumina support (1/12 in. extrusions) was ground to a fine powder prior to use. Following impregnation, the catalysts were dried for 24 h at 393 K and then calcined for 3 h in air at 773 K.

The catalyst synthesis apparatus consisted of an atmospheric pressure flow system outfitted with a quartz U-tube type reactor (15 mm OD), stainless steel gas manifold, mass flow controllers (MKS Instruments), and a furnace, composed of a ceramic fiber heater (Watlow) and a temperature controller (Watlow). The synthesis procedures for alumina-supported β-Mo_2C and γ-Mo_2N catalysts, hereafter referred to as Mo_2C/Al_2O_3 and Mo_2N/Al_2O_3 catalysts, respectively, have been described in detail elsewhere (12). Synthesis of alumina-supported α-$MoC_{(1-x)}$ ($x \approx 0.5$) catalysts, hereafter referred to as $MoC_{(1-x)}/Al_2O_3$ catalysts, followed the procedure outlined by Lee and co-workers (15, 20). A typical synthesis employed 1.0 g of MoO_3/Al_2O_3 supported on a plug of quartz wool; the oxide precursor was outgassed for 1 h at 673 K in a 30 sccm/min flow of He (Airco, 99.999%) prior to switching to a 60 sccm/min flow of anhydrous ammonia (Airco, 99.99%). Temperature programmed reduction (TPR) of the oxide precursor was carried out from 673 to 970 K at a heating rate of 30 K/h. The resulting Mo_2N/Al_2O_3 catalyst was then cooled to room temperature in a 30 sccm/min flow of He, following which a second TPR program was carried out from 673 to 950 K in a 60 sccm/min flow of a 20 mol% CH_4/H_2 mixture (Airco, CH_4 99%, H_2 99.97%). The resulting $MoC_{(1-x)}/Al_2O_3$ catalyst was cooled to room temperature in a 30 sccm/min flow of He and then passivated in a 30 sccm/min flow of a 1% O_2/He mixture (Airco) at 298 K for 3 h prior to removal from the flow system. The He and CH_4/H_2 mixture were purified prior to use by passing through 5A molecular sieve (Alltech) and O_2 (Oxyclear) purification traps. Bulk Mo carbide and nitride catalysts were prepared by the same synthesis procedures employed for the alumina-supported catalysts starting with bulk MoO_3 (Alfa Aesar, 99.998%). Sulfided Mo/Al_2O_3 catalysts were synthesized *in situ*. Following outgassing in flowing He at 673 K, oxidic precursors were sulfided in a 60 sccm/min flow of a 3.03% H_2S/H_2 mixture (Airco) at 623 K for 2 h.

X-Ray Diffraction Measurements

X-ray diffraction patterns were acquired for bulk and alumina-supported Mo carbide and nitride catalysts using the packed powder method. Catalyst samples were passivated as described in the catalyst preparation section prior to transferring to the X-ray diffractometer. Diffraction patterns were acquired using a Rigaku Geigerflex diffractometer and Cu Kα radiation ($\lambda = 1.5418$ Å) and are reproduced here without any background or smoothing treatment.

BET and Pulsed Chemisorption Measurements

BET surface area and pulsed chemisorption (CO and O_2) measurements were carried out using a Micromeritics Pulse Chemisorb 2700 apparatus. For both types of measurements, catalyst samples (~0.10 g) were placed in a quartz U-tube (15 mm OD), where they were degassed in flowing He (45 sccm/min) at 673 K for 2 h. Supported molybdenum carbide and nitride catalysts were then activated by heating to 750 K for 2 h in a 60 sccm/min flow of H_2. Sulfided Mo/Al_2O_3 catalysts were prepared as described above and subsequently reduced at 623 K in a 60 sccm/min flow of H_2 for 1 h. Additional experiments were carried out for Mo carbide and nitride catalysts sulfided prior to the chemisorption measurement. The Mo_2C/Al_2O_3, $MoC_{(1-x)}/Al_2O_3$ and Mo_2N/Al_2O_3 catalysts were sulfided *in situ* (60 sccm/min flow of a 3.03% H_2S/H_2 mixture at 623 K for 2 h) followed by reduction in flowing H_2 at 623 K for 1 h. Prior to the BET and chemisorption measurements, the Mo carbide, nitride, and sulfided Mo catalysts were subjected to a final outgassing treatment in which they were heated to 673 K in flowing He (45 sccm/min) for 1 h. The He and H_2 used in the chemisorption system were passed through 5A molecular sieve and O_2 purification traps prior to use.

Single point BET surface area measurements were carried out using a 28.6% N_2/He mixture (Airco). The instrument was calibrated prior to the BET measurements using pure N_2 gas.

Chemisorption capacities were measured by injecting a calibrated sample loop of gas, CO (Airco, 99.99%) or O_2 (Airco, 10.3% in He), at one minute intervals into an He

flow (45 sccm/min for CO, 15 sccm/min for O_2) passing over the catalysts until gas uptake ceased. Prior to injection, the CO was passed through a coil of $\frac{1}{8}$-inch stainless steel tubing submerged in a pentane slush to remove metal carbonyl impurities. Carbon monoxide and O_2 chemisorption studies were performed at 273 and 196 K, respectively. Fresh catalyst samples were prepared for each chemisorption measurement.

Thiophene HDS Activity Measurements

Thiophene HDS activity measurements were carried out using an atmospheric pressure flow reactor outfitted with a gas chromatograph (HP 5890 Series II) equipped with a flame ionization detector for on-line analysis of thiophene and hydrocarbon products. The flow reactor system has been described in detail elsewhere (12). Catalyst samples (∼0.10 g) were supported on a quartz wool plug in a quartz U-tube reactor (15 mm OD) in a 50 sccm/min flow of a 1.8 mol% thiophene/H_2 mixture prepared by means of a two-stage thiophene bubbler apparatus. The thiophene used in this study (Aldrich Chemical Co., 99+%) was purified according to the procedure of Spies and Angelici (21) prior to use in order to remove thiol impurities. The reaction temperature was maintained using a ceramic-fiber furnace (Watlow) outfitted with a programmable temperature controller (Omega). Supported Mo carbide and nitride catalysts were degassed in a 60 sccm/min flow of He at 673 K for 1 h, activated in a 60 sccm/min flow of H_2 at 750 K for 2 h, and then cooled to the desired reaction temperature prior to switching to the thiophene/H_2 flow. Sulfided Mo/Al_2O_3 catalysts were prepared as described above, outgassed in flowing He (60 sccm/min) at the desired reaction temperature for 10 min and the flow then switched to the thiophene/H_2 mixture. Thiophene HDS conversion data were collected at 1 h intervals over 24 h at a reaction temperature of 693 K. Steady state conversion was achieved after ∼16 h; catalyst activities reported here are the values after 24 h on-stream. The major HDS products (butadiene, 1-butene, *cis*-2-butene, *trans*-2 butene, and butane) and unreacted thiophene were separated using a 30-m GS-Alumina column (J & W Scientific). C_1–C_3 hydrocarbons totalled <1% of the products. The detector response for the C_4 hydrocarbon products was calibrated with analytical gas standards (Scott) to facilitate conversion calculations.

RESULTS

The Mo carbide and nitride catalysts investigated in this study were subjected to different pretreatment conditions depending upon the particular experiment. X-ray diffraction analyses of Mo_2C/Al_2O_3, $MoC_{(1-x)}/Al_2O_3$, and Mo_2N/Al_2O_3 catalysts were carried out using prepared catalyst samples which were passivated in a 1% O_2/He mixture prior to removal from the synthesis apparatus. Chemisorption measurements were carried out for both freshly reduced and sulfided Mo carbide and nitride catalysts. To avoid confusion, catalysts subjected to the sulfidation procedure will be referred to as sulfided catalysts (e.g., *sulfided* Mo_2C/Al_2O_3). Lastly, thiophene HDS activity measurements of Mo_2C/Al_2O_3, $MoC_{(1-x)}/Al_2O_3$, and Mo_2C/Al_2O_3 catalysts were carried out using catalyst samples which were reduced in flowing H_2 to remove the passivating layer of oxygen adsorbed following synthesis. Results described elsewhere (12) indicate that the surfaces of working Mo carbide and nitride catalysts resemble those of catalysts subjected to the sulfidation procedure.

X-Ray Diffraction Analysis of Alumina-Supported Mo Carbide and Nitride Catalysts

X-ray diffraction analysis was carried out for bulk and alumina-supported molybdenum carbide and nitride catalysts with a range of Mo loadings and diffraction patterns for catalysts with 10, 20, 30, and 48 wt% Mo loadings are shown in Figs. 2–4. For Mo loadings below ∼25 wt%, only diffraction peaks associated with the γ-Al_2O_3 support are apparent. At higher loadings, the X-ray diffraction patterns for the alumina-supported catalysts display a number of diffraction peaks observed for the corresponding bulk Mo containing phase. The diffraction pattern for Mo_2C/Al_2O_3 catalysts with loadings of 30 wt% and above (Fig. 2) show peaks at 34.7°, 38.0°, 39.8°, 62.1°, and 75.5° which can be assigned to the {100}, {002}, {101}, {110} reflections and an unresolved doublet band assigned to the {112} and {201} reflections of bulk β-Mo_2C, respectively (22). Additional peaks at 52.5° and 69.9° are observed for the 48 wt% Mo_2C/Al_2O_3 catalyst which correspond to the {102} and {103} reflections, respectively, of bulk β-Mo_2C (22). For $MoC_{(1-x)}/Al_2O_3$ catalysts, the X-ray diffraction patterns for catalysts with Mo loadings of 30 wt% and above (Fig. 3) exhibit peaks at 37.3°, 43.3°, 62.5°, and 74.8° which can be assigned to the {111}, {200}, {220}, and {311} reflections, respectively, of bulk α-$MoC_{(1-x)}$ ($x \approx 0.5$) (23). For the 48 wt% $MoC_{(1-x)}/Al_2O_3$ catalyst, an additional peak is apparent at 78.6° which can be assigned to the {222} reflection of bulk α-$MoC_{(1-x)}$ ($x \approx 0.5$) (23). The diffraction patterns for Mo_2N/Al_2O_3 catalysts with Mo loadings of 30 wt% and above (Fig. 4) exhibit peaks at 38.2°, 44.2°, 64.0°, and 76.7° which are assigned to the {111}, {200}, {220}, and {311} reflections of bulk γ-Mo_2N, respectively (24). Using the Scherrer equation and the width at half height of the {101}, {200}, and {200} reflections for the Mo_2C/Al_2O_3, $MoC_{(1-x)}/Al_2O_3$, and Mo_2N/Al_2O_3 catalysts, respectively, with 30 wt% Mo loadings, particle sizes of ∼60 Å can be estimated for the supported Mo containing phases. The X-ray diffraction patterns for the supported Mo carbide and nitride catalysts shown in Figs. 2–4 are consistent with those

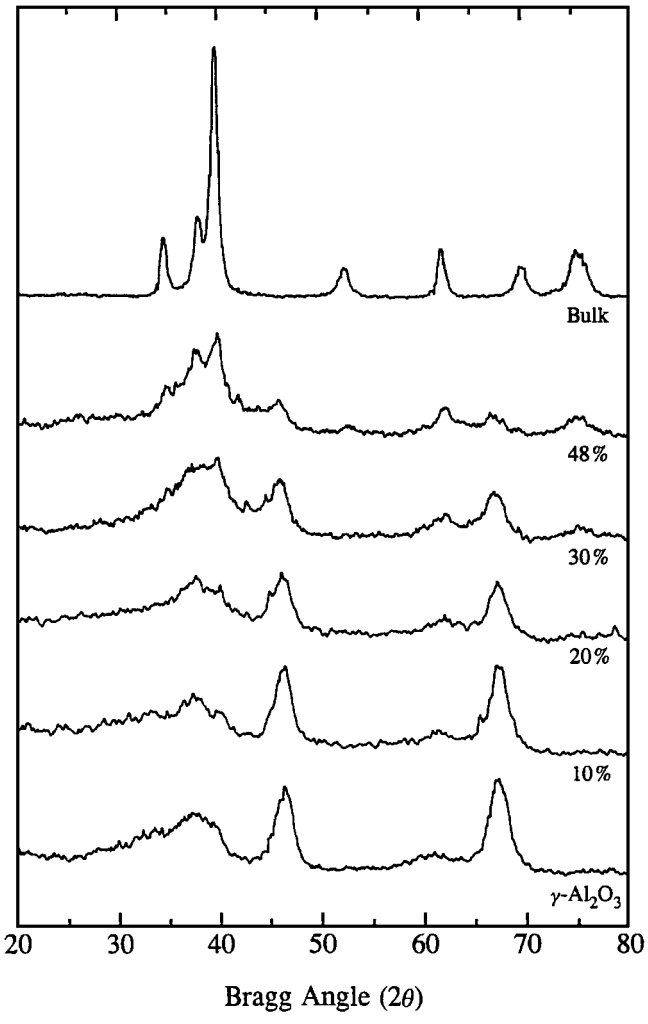

FIG. 2. X-ray diffraction patterns of Mo_2C/Al_2O_3 catalysts with different Mo loadings. X-ray patterns of γ-Al_2O_3 and bulk β-Mo_2C are included for reference purposes.

obtained by others for Mo_2C/Al_2O_3 (20), $MoC_{(1-x)}/Al_2O_3$ (20), and Mo_2N/Al_2O_3 catalysts (8).

BET Surface Areas and Chemisorption Capacities of Alumina-Supported Mo Carbide and Nitride Catalysts

The BET surface areas of Mo_2C/Al_2O_3, $MoC_{(1-x)}/Al_2O_3$, Mo_2N/Al_2O_3, and sulfided Mo/Al_2O_3 catalysts with Mo loadings in the range 1.5–20 wt% are listed in Tables 1–4. The surface areas of the catalysts decrease monotonically with increased Mo loading and, for a given loading, are similar for the Mo carbide, nitride, and sulfided Mo catalysts.

The carbon monoxide and oxygen chemisorption capacities for freshly activated Mo_2C/Al_2O_3, $MoC_{(1-x)}/Al_2O_3$, and Mo_2N/Al_2O_3 catalysts are listed in Tables 1–3. The chemisorption capacities measured for these catalysts are similar in magnitude, but somewhat lower than those obtained by others (2, 3, 8, 15, 20, 26, 27). This discrepancy is due to the fact that our catalysts have been passivated in a 1% O_2/He flow following synthesis and then reactivated in flowing H_2 prior to the chemisorption measurements, while others typically measure chemisorption capacities directly after synthesis. As discussed elsewhere (12), the CO chemisorption capacities of Mo_2C/Al_2O_3 catalysts submitted to the passivation/activation process are approximately one-half those of the freshly synthesized catalysts. This is believed to be due to the fact that oxygen adsorbed onto the β-Mo_2C particles during passivation cannot be completely removed by activation in flowing H_2.

The CO and O_2 chemisorption capacities for reduced Mo_2C/Al_2O_3 catalysts are plotted in Fig. 5 as a function of the Mo loading. The chemisorption capacities of the freshly reduced Mo_2C/Al_2O_3 catalysts increase rapidly for Mo

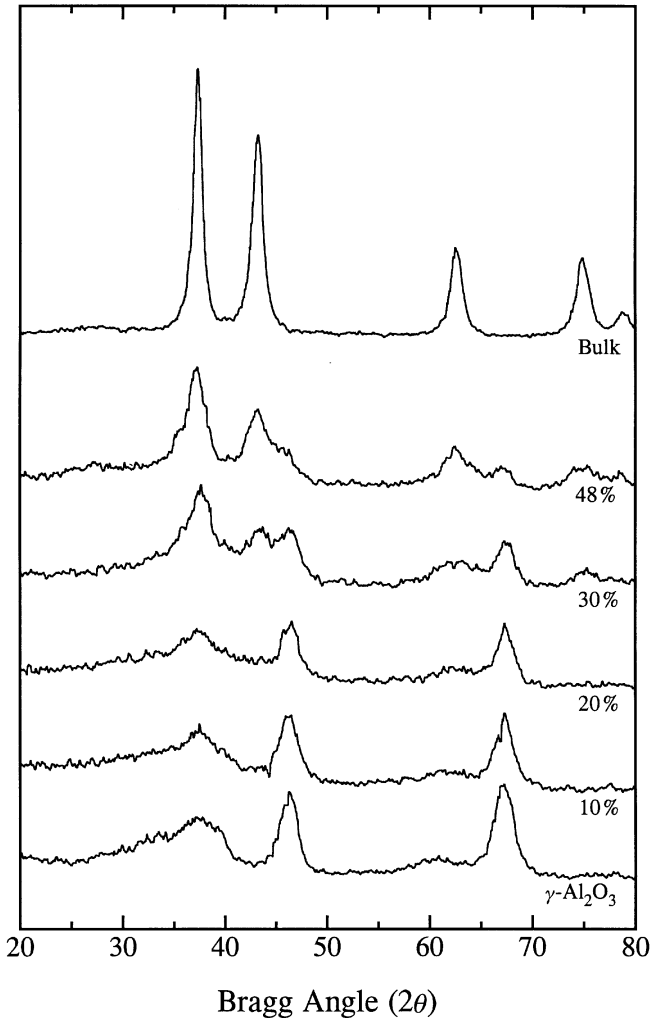

FIG. 3. X-ray diffraction patterns of $MoC_{(1-x)}/Al_2O_3$ catalysts with different Mo loadings. X-ray patterns of γ-Al_2O_3 and bulk α-$MoC_{(1-x)}$ ($x \approx 0.5$) are included for reference purposes.

TABLE 1

Catalytic Data for Mo_2C/Al_2O_3 Catalysts

Mo loading (wt%)	Surface area (m^2/g)	CO chemisorption capacity (273 K)		O_2 chemisorption capacity (196 K)		Thiophene HDS activity[a]	
		Reduced (μmol/g)	Sulfided (μmol/g)	Reduced (μmol/g)	Sulfided (μmol/g)	nmol Th/g/s	μmol Th/mol Mo/s
1.5	210	2.7	7.1	11.7	8.2	108	693
2.5	209	7.3	16.1	31.8	12.2	229	881
5.0	195	28.0	23.2	48.0	25.3	486	936
7.5	201	47.3	33.7	91.8	39.0	727	935
10.0	189	69.0	53.0	111	57.0	923	891
12.5	177	76.7	60.8	129	69.0	991	766
15.0	179	82.6	70.2	128	66.0	1126	727
17.5	171	81.4	62.0	108	73.0	1080	599
20.0	164	90.9	69.7	116	56.2	1006	489

[a] Measured after 24 h at 693 K.

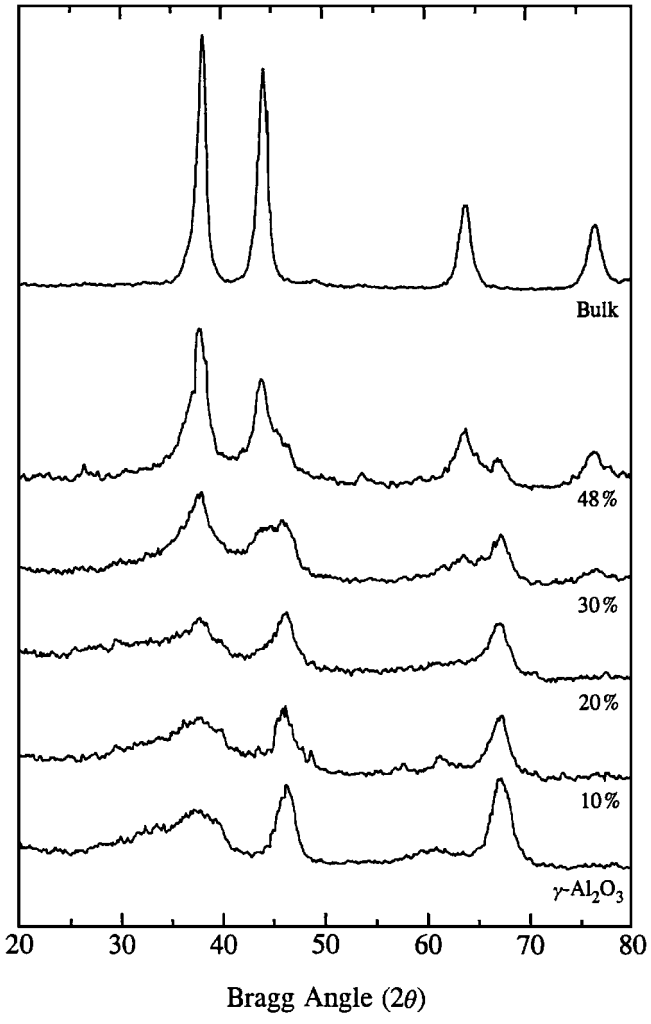

FIG. 4. X-ray diffraction patterns of Mo_2N/Al_2O_3 catalysts with different Mo loadings. X-ray patterns of γ-Al_2O_3 and bulk γ-Mo_2N are included for reference purposes.

loadings up to 12.5–15 wt%, above which the chemisorption capacities begin to plateau. Similar behavior is observed for the $MoC_{(1-x)}/Al_2O_3$ and Mo_2N/Al_2O_3 catalysts. The plateau of the chemisorption capacities for Mo loadings above 12.5–15 wt% is consistent with the results of a study in our laboratory of the molybdena coverage in MoO_3/Al_2O_3 catalysts in which the saturation coverage of MoO_3 on γ-Al_2O_3 was observed to be 15 wt% ($(42 \pm 3) \times 10^{13}$ Mo atoms/cm^2) (25). The fact that the trend of chemisorption capacities of the alumina-supported carbide and nitride catalysts mirrors that of the precursor MoO_3 coverage indicates that insignificant sintering of the Mo containing overlayer occurs during the high temperature synthesis of the carbide and nitride catalysts.

Chemisorption capacities were also measured for *sulfided* Mo_2C/Al_2O_3, $MoC_{(1-x)}/Al_2O_3$, and Mo_2N/Al_2O_3 catalysts prepared as described in the experimental section. These data are listed in Tables 1–3 and, for the Mo_2C/Al_2O_3 catalysts, are plotted in Fig. 5. Sulfidation of the carbide and nitride catalysts, shown in earlier work from our laboratory to be limited to the exterior of the supported carbide and nitride particles, causes a significant decrease in the chemisorption capacities of the catalysts for most Mo loadings. For comparison purposes, CO and O_2 chemisorption capacities were also measured for sulfided Mo/Al_2O_3 catalysts, prepared using the same sulfiding conditions employed for the carbide and nitride catalysts. The chemisorption data for the sulfided Mo/Al_2O_3 catalysts, plotted versus Mo loading, are also shown in Fig. 5. Comparison of the chemisorption data for the *sulfided* Mo_2C/Al_2O_3 and Mo/Al_2O_3 catalysts reveals an important trend. For almost every loading, the *sulfided* Mo_2C/Al_2O_3 catalysts have higher CO and O_2 chemisorption capacities than the corresponding sulfided Mo/Al_2O_3 catalysts. This trend holds true for the *sulfided* $MoC_{(1-x)}/Al_2O_3$ and Mo_2N/Al_2O_3 catalysts as well, except for the singular case of O_2 chemisorption

TABLE 2

Catalytic Data for $MoC_{(1-x)}/Al_2O_3$ Catalysts

Mo loading (wt%)	Surface area (m^2/g)	CO chemisorption capacity (273 K)		O_2 chemisorption capacity (196 K)		Thiophene HDS activity[a]	
		Reduced (μmol/g)	Sulfided (μmol/g)	Reduced (μmol/g)	Sulfided (μmol/g)	nmol Th/g/s	μmol Th/mol Mo/s
1.5	208	7.3	7.6	8.8	9.7	93	597
2.5	206	8.4	9.5	14.9	12.0	144	553
5.0	197	33.8	15.8	40.2	22.2	356	685
7.5	190	36.5	36.1	54.3	39.7	530	682
10.0	183	48.5	51.5	69.8	40.7	667	643
12.5	180	65.8	67.1	82.3	49.0	694	536
15.0	176	89.2	68.9	103	54.3	721	465
17.5	173	94.4	67.8	107	56.9	793	440
20.0	155	92.0	71.4	113	55.4	860	418

[a] Measured after 24 h at 693 K.

capacities of *sulfided* $MoC_{(1-x)}/Al_2O_3$ catalysts which are almost identical to those of the sulfided Mo/Al_2O_3 catalysts.

Thiophene HDS Activities of Alumina-Supported Mo Carbide and Nitride Catalysts

Thiophene HDS activity measurements were carried out for Mo_2C/Al_2O_3, $MoC_{(1-x)}/Al_2O_3$, Mo_2N/Al_2O_3, and sulfided Mo/Al_2O_3 catalysts with Mo loadings in the range 1.5–20 wt%. The γ-Al_2O_3 support used in this study was inactive for thiophene HDS. At a reaction temperature of 693 K, steady state activity was achieved for the Mo carbide, nitride and sulfided Mo catalysts after ~16 h; thiophene HDS activities after 24 h on-stream are listed in Tables 1–4 and are plotted as a function of Mo loading in Figs. 6–8. The HDS activities of the sulfided Mo/Al_2O_3 catalysts are shown in each of the figures for comparison purposes. The product distributions for the Mo_2C/Al_2O_3, $MoC_{(1-x)}/Al_2O_3$, Mo_2N/Al_2O_3, and sulfided Mo/Al_2O_3 catalysts are similar and are nearly identical to those for catalysts with 10 wt% Mo loadings which have been discussed elsewhere (12).

In order to make a direct comparison of the thiophene HDS activities of the Mo carbide, nitride and sulfided Mo catalysts, relative HDS activities were calculated using Eq. [1], where A_i(carb) (or A_i(nitr)) and A_i(sulf) are the HDS activities per gram of catalyst of the supported Mo carbide (or nitride) and sulfided Mo catalysts, respectively:

$$\text{Relative HDS activity} = \frac{1}{N}\sum_{i=1}^{n} W_i \frac{A_i(\text{carb})}{A_i(\text{sulf})}. \qquad [1]$$

The weighting factor, W_i, and normalization factor, N, are defined in Eq. [2]:

$$W_i = \frac{1}{2}\left(\frac{A_i(\text{carb})}{A_{\max}(\text{carb})} + \frac{A_i(\text{sulf})}{A_{\max}(\text{sulf})}\right); \quad N = \sum_{i=1}^{n} W_i. \qquad [2]$$

TABLE 3

Catalytic Data for Mo_2N/Al_2O_3 Catalysts

Mo loading (wt%)	Surface area (m^2/g)	CO chemisorption capacity (273 K)		O_2 chemisorption capacity (196 K)		Thiophene HDS activity[a]	
		Reduced (μmol/g)	Sulfided (μmol/g)	Reduced (μmol/g)	Sulfided (μmol/g)	nmol Th/g/s	μmol Th/mol Mo/s
1.5	208	12.7	7.2	16.3	4.5	94	601
2.5	209	11.9	7.9	9.2	8.2	229	882
5.0	203	35.7	23.1	47.9	20.0	298	574
7.5	194	67.9	40.7	70.2	53.6	555	713
10.0	193	78.0	49.0	115	59.0	668	646
12.5	188	91.4	65.1	80.9	64.7	1002	776
15.0	188	108	61.6	99.1	56.0	942	609
17.5	193	111	72.1	109	66.7	1099	610
20.0	160	142	74.0	129	57.9	878	427

[a] Measured after 24 h at 693 K.

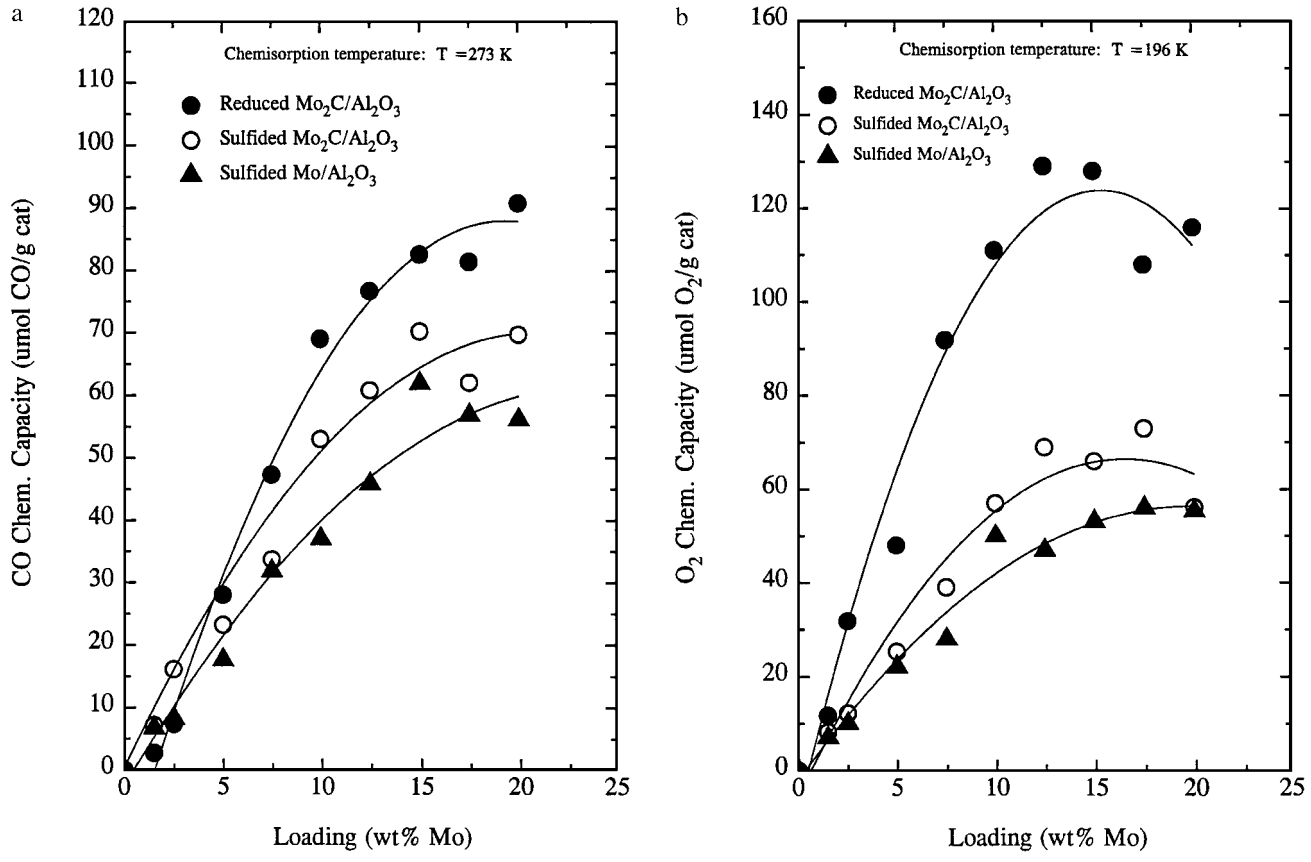

FIG. 5. (a) CO and (b) O_2 chemisorption capacities for reduced and sulfided Mo_2C/Al_2O_3 catalysts, as well as sulfided Mo/Al_2O_3 catalysts with Mo loadings in the range 1.5–20 wt%.

Equation [1] determines a weighted average of the HDS activity of the Mo carbide (or nitride) catalysts divided by the HDS activity of the sulfided Mo catalysts for the entire range of Mo loadings (1.5–20 wt%). This equation gives the heaviest weighting to the catalysts with the highest HDS activities and was chosen for two reasons. The lowest HDS activities have the highest relative uncertainties and, therefore, the ratio A_i(carb)/A_i(sulf) is the most uncertain for these catalysts (i.e., low Mo loadings). Also, it is the HDS activities for catalysts with the highest HDS activities (i.e., $\geq$10 wt% Mo) which are of the greatest interest for the commercial HDS process.

The relative HDS activities ($\pm$ one std. dev.) of the Mo_2C/Al_2O_3, $MoC_{(1-x)}/Al_2O_3$, Mo_2N/Al_2O_3, and sulfided Mo/Al_2O_3 catalysts calculated using Eq. [1] are listed in Table 5. The HDS activities of the catalysts increase according to the trend: sulfided Mo $\approx$ $MoC_{(1-x)}$ < Mo_2N < Mo_2C and are consistent with our earlier results for Mo_2C/Al_2O_3, Mo_2N/Al_2O_3, and sulfided Mo/Al_2O_3 catalysts with 10 wt% Mo loadings. The observation that $MoC_{(1-x)}/Al_2O_3$ catalysts have significantly lower HDS activities than Mo_2C/Al_2O_3

TABLE 4

Catalytic Data for Sulfided Mo/Al_2O_3 Catalysts

Mo loading (wt%)	Surface area (m^2/g)	Chemisorption capacity CO (273 K) (μmol/g)	Chemisorption capacity O_2 (196 K) (μmol/g)	Thiophene HDS activity[a] nmol Th/g/s	Thiophene HDS activity[a] μmol Th/mol Mo/s
1.5	212	6.7	7.0	107	688
2.5	219	8.2	10.0	207	804
5.0	214	17.6	22.1	358	704
7.5	202	31.8	28.0	555	736
10.0	196	37.0	50.0	587	591
12.5	192	45.8	46.9	684	558
15.0	178	61.9	51.9	744	512
17.5	171	56.8	56.0	778	464
20.0	157	56.1	55.4	746	394

[a] Measured after 24 h at 693 K.

TABLE 5

Relative HDS Activities

Catalyst	Relative HDS activity
Sulfided Mo/Al_2O_3	1.00
Mo_2C/Al_2O_3	1.41 ± 0.13
$MoC_{(1-x)}/Al_2O_3$	1.02 ± 0.11
Mo_2N/Al_2O_3	1.22 ± 0.20

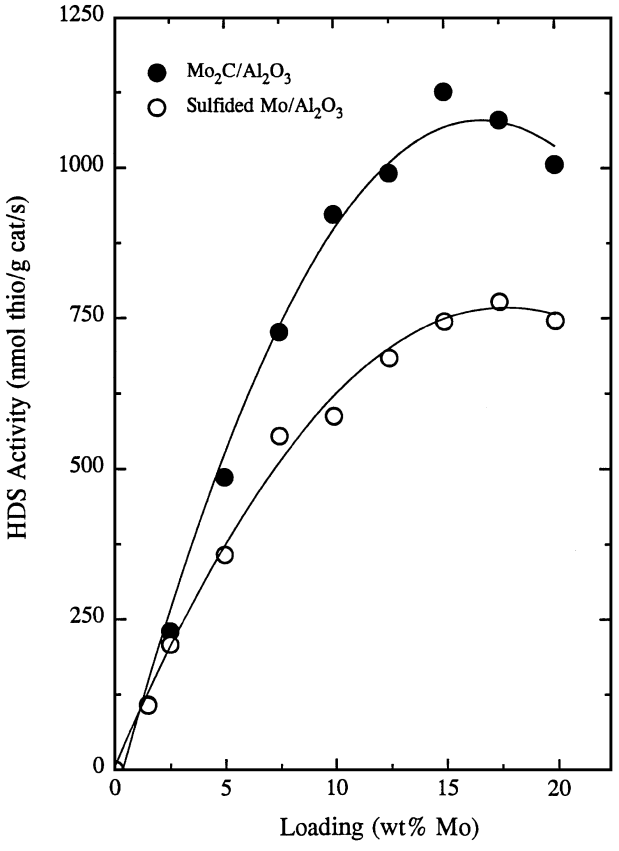

FIG. 6. Thiophene HDS activities for Mo_2C/Al_2O_3 and sulfided Mo/Al_2O_3 catalysts with Mo loadings in the range 1.5–20 wt%.

catalysts was unexpected. Ranhotra *et al.* observed structure sensitivity in the case of ethane hydrogenolysis over molybdenum carbide with bulk β-Mo_2C over 200 times more active the α-$MoC_{(1-x)}$ (30). Structure sensitivity has also been invoked by Thompson and co-workers to explain the dependence of the rate of pyridine HDN on particle size for bulk and alumina-supported γ-Mo_2N (6, 8). As will be discussed shortly, it is unclear whether structure sensitivity is responsible for the different thiophene HDS activities measured in this study for Mo_2C/Al_2O_3 and $MoC_{(1-x)}/Al_2O_3$ catalysts.

Correlation of Thiophene HDS Activity with the CO and O_2 Chemisorption Capacities of Alumina-Supported Mo Carbide, Nitride, and Sulfided Mo Catalysts

In Figs. 9–11, the thiophene HDS activities of Mo_2C/Al_2O_3, $MoC_{(1-x)}/Al_2O_3$, Mo_2N/Al_2O_3, and sulfided Mo/Al_2O_3 catalysts are plotted as functions of their CO and O_2 chemisorption capacities. The chemisorption capacities used for these plots are those of catalysts *sulfided prior to the chemisorption measurements* as earlier studies in our laboratory indicated that the surfaces of Mo_2C/Al_2O_3 and Mo_2N/Al_2O_3 catalysts are sulfided under HDS reaction conditions (12). Similar results have also been obtained

TABLE 6

Thiophene HDS Turnover Frequencies

Catalyst	Turnover frequency: Based upon titration of sites with CO	Turnover frequency: Based upon titration of sites with O_2
Sulfided Mo/Al_2O_3	0.012 ± 0.001 s^{-1}	0.013 ± 0.001 s^{-1}
Mo_2C/Al_2O_3	0.015 ± 0.001	0.015 ± 0.001
$MoC_{(1-x)}/Al_2O_3$	0.011 ± 0.001	0.015 ± 0.001
Mo_2N/Al_2O_3	0.014 ± 0.001	0.014 ± 0.002

for $MoC_{(1-x)}/Al_2O_3$ catalysts (31). A linear correlation is observed between thiophene HDS activity and chemisorption capacity for the Mo carbide, nitride, and sulfided Mo catalysts for the range of Mo loading (1.5–20 wt% Mo) investigated. Linear regression was carried out for each set of data and the slopes of the best-fit lines are the thiophene HDS turnover frequencies for the different catalysts. The turnover frequencies ($\pm$ one std. dev.) are listed in Table 6; the turnover frequencies are very tightly grouped for the Mo carbide, nitride, and sulfided Mo catalysts.

The turnover frequencies determined in this study for sulfided Mo/Al_2O_3 catalysts can be compared with values calculated using the data of Bachelier *et al.* (18, 32).

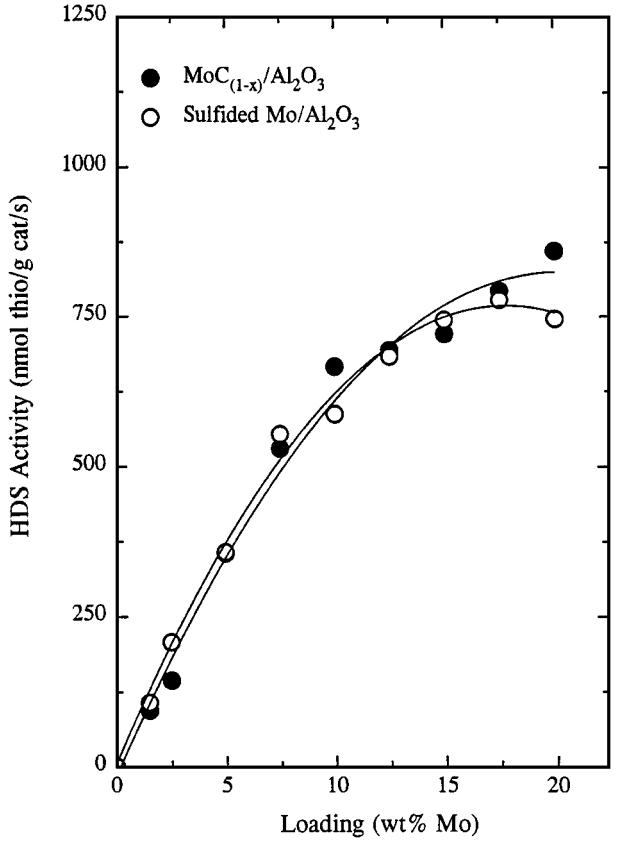

FIG. 7. Thiophene HDS activities for $MoC_{(1-x)}/Al_2O_3$ and sulfided Mo/Al_2O_3 catalysts with Mo loadings in the range 1.5–20 wt%.

Working at the same reaction temperature of 693 K, these researchers observed a linear relationship between thiophene HDS activity and chemisorption capacity for molybdenum loadings up to 10 wt%. Thiophene HDS turnover frequencies of 0.024 ± 0.001 s^{-1} and 0.0046 ± 0.0002 s^{-1} are calculated based upon titration of sites by CO (273 K) and O_2 (333 K) chemisorption, respectively. The higher turnover frequency determined by Bachelier *et al.* based upon CO titration of sites is probably due to the higher thiophene pressure ($P_{Th} = 60$ Torr) used in their HDS activity measurements than was used in our work ($P_{Th} = 13.7$ Torr). The discrepancy between the turnover frequencies determined using O_2 chemisorption capacities determined by Bachelier *et al.* and in our laboratory can be traced to the different conditions under which the chemisorption measurements were performed. Bachelier *et al.* carried out their O_2 chemisorption measurements at 333 K while a temperature of 196 K was utilized in our measurements. Studies by Massoth and co-workers (17) indicate that O_2 chemisorption on sulfided Mo/Al_2O_3 catalysts at temperatures above 196 K overestimates the number of adsorption sites on these catalysts. Slow oxidation of alumina-supported sulfided Mo particles was found to occur at 273 and 297 K which resulted in a significantly higher uptake of O_2.

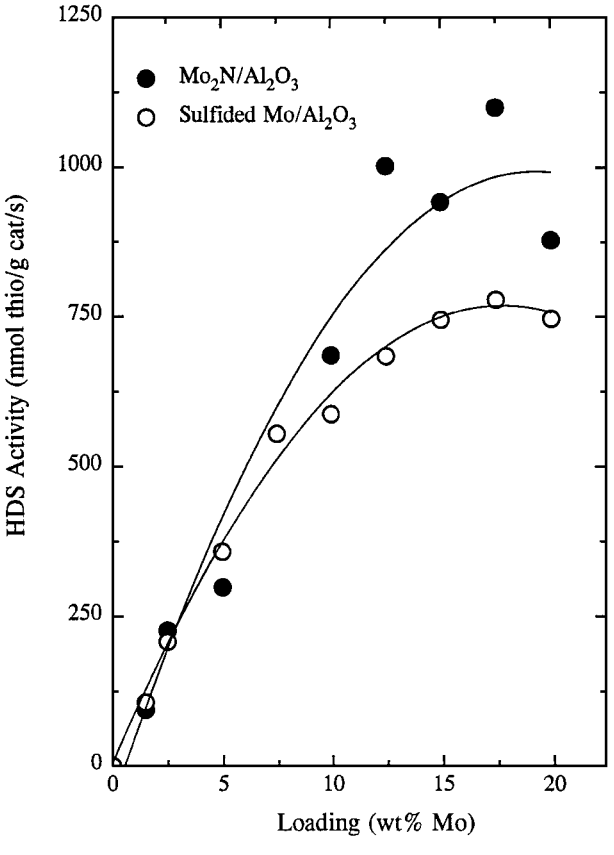

FIG. 8. Thiophene HDS activities for Mo_2N/Al_2O_3 and sulfided Mo/Al_2O_3 catalysts with Mo loadings in the range 1.5–20 wt%.

Excluding our recently reported turnover frequencies for Mo_2C/Al_2O_3, $MoC_{(1-x)}/Al_2O_3$, Mo_2N/Al_2O_3, and sulfided Mo/Al_2O_3 catalysts with 10 wt% Mo loadings (12), a search of the literature produced only one report of a thiophene HDS turnover frequency for a molybdenum carbide or nitride catalyst. Lee and Boudart (9) determined an initial turnover frequency of slightly less than 0.001 s^{-1} for unsupported $MoC_{(1-x)}$ at a temperature of 573 K. These authors used room temperature CO chemisorption to estimate the number of active sites on the unsupported molybdenum carbide catalyst.

DISCUSSION

The primary goals of this study were twofold: (1) to make a direct comparison of the HDS catalytic properties of alumina-supported Mo carbide, nitride, and sulfided Mo catalysts; and (2) to test a previously proposed model which suggests that the higher HDS activity of Mo carbide and nitride catalysts when compared to conventional sulfided Mo catalysts is due to a higher density of active sites on a thin sulfided Mo layer located at the surface of the supported carbide and nitride particles. To address these goals, thiophene HDS activities were measured for Mo_2C/Al_2O_3, $MoC_{(1-x)}/Al_2O_3$, Mo_2N/Al_2O_3, and sulfided Mo/Al_2O_3 catalysts with Mo loadings in the range 1.5–20 wt%, and the catalyst activities were correlated with the CO and O_2 chemisorption capacities of the catalysts.

For the wide range of loadings investigated, the thiophene HDS activities of the Mo carbide, nitride, and sulfided Mo catalysts, normalized per gram of catalyst or mole Mo, were observed to increase according to the trend: sulfided Mo $\approx MoC_{(1-x)} < Mo_2N < Mo_2C$. Importantly, Mo_2C/Al_2O_3 and Mo_2N/Al_2O_3 catalysts were observed to have significantly higher thiophene HDS activities than conventional sulfided Mo/Al_2O_3 catalysts; these results suggest that the Mo_2C and Mo_2N catalysts have strong potential for use in the commercial hydrodesulfurization process. In contrast, $MoC_{(1-x)}/Al_2O_3$ catalysts were observed to have HDS activities similar to those of the corresponding sulfided Mo/Al_2O_3 catalysts. Some insight into the different HDS catalytic properties of alumina-supported β-Mo_2C and α-$MoC_{(1-x)}$ ($x \approx 0.5$) determined in this study can be gained from examination of the chemisorption properties of the catalysts; this will be addressed shortly.

As reported in an earlier study (12), X-ray diffraction and IR spectroscopy experiments in our laboratory indicate that a thin layer of sulfided Mo forms at the surface Mo_2C/Al_2O_3 and Mo_2N/Al_2O_3 catalysts under HDS reaction conditions as depicted in Fig. 1. Similar results have been obtained for $MoC_{(1-x)}/Al_2O_3$ catalysts as well (31). The IR spectroscopy results obtained in the earlier study indicate that the adsorption sites on alumina-supported Mo carbide and nitride catalysts under HDS conditions are essentially identical

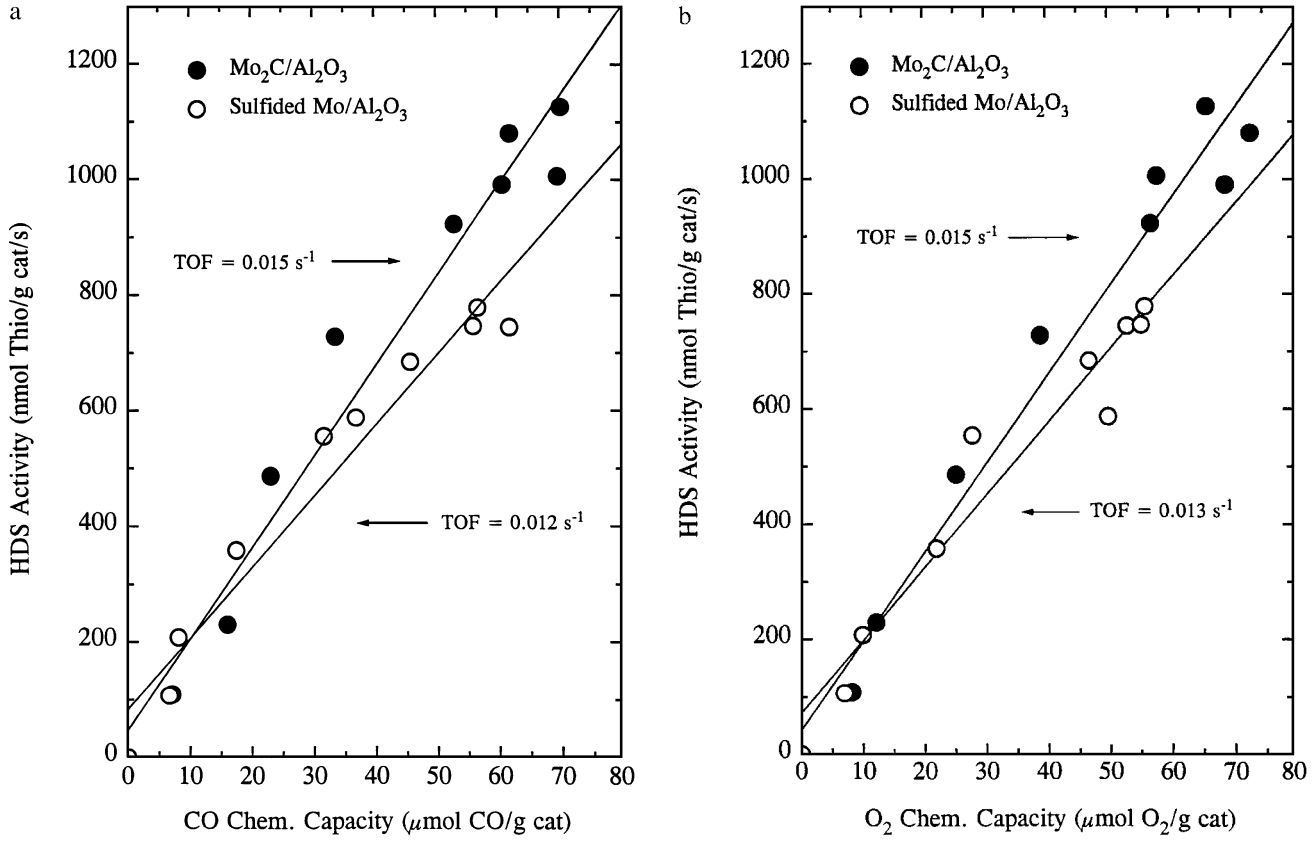

FIG. 9. Correlation of thiophene HDS activity with (a) CO and (b) O_2 chemisorption capacities for Mo_2C/Al_2O_3 and sulfided Mo/Al_2O_3 catalysts with Mo loadings in the range 1.5–20 wt%.

to those on sulfided Mo/Al_2O_3 catalysts (12). Additionally, the product distributions for thiophene HDS over Mo_2C/Al_2O_3, $MoC_{(1-x)}/Al_2O_3$, Mo_2N/Al_2O_3, and sulfided Mo/Al_2O_3 catalysts are similar, suggesting that the mechanism of the reaction is the same for the different catalysts (12, 31).

The data presented in this study provide considerable evidence that the higher thiophene HDS activity of Mo_2C/Al_2O_3 and Mo_2N/Al_2O_3 catalysts when compared to sulfided Mo/Al_2O_3 catalysts can be traced to a higher density of active sites on the Mo_2N and Mo_2C catalysts than on the sulfided Mo catalysts. This conclusion is supported by the chemisorption data presented in Tables 1–4. Whether freshly activated in flowing H_2 or sulfided in a flowing H_2S/H_2 mixture, Mo_2C/Al_2O_3 and Mo_2N/Al_2O_3 catalysts have consistently higher CO and O_2 chemisorption capacities than sulfided Mo/Al_2O_3 catalysts over the range of Mo loadings 1.5–20 wt%. Because alumina-supported Mo carbide and nitride catalysts become sulfided under HDS conditions, we believe the chemisorption capacities of Mo_2C/Al_2O_3, $MoC_{(1-x)}/Al_2O_3$, Mo_2N/Al_2O_3 *which are sulfided prior to the chemisorption measurement* provide the best estimate of the number of active sites for thiophene HDS at the catalyst surfaces (12).

A number of studies in recent years have shown that there is a linear correlation between the thiophene HDS activity of sulfided Mo/Al_2O_3 catalysts and their CO (32), NO (33–36), and O_2 (18, 32, 37) chemisorption capacities. Our results provide additional confirmation of this relationship and further suggest that CO chemisorption at 273 K and O_2 chemisorption at 196 K are equivalent measures of active sites on sulfided Mo/Al_2O_3 catalysts. The chemisorption capacities for the two probe molecules on sulfided Mo/Al_2O_3 catalysts at the given temperatures are quite similar and the turnover frequencies determined from the slopes of the linear regressions (see Fig. 9 and Table 6) are the same within one standard deviation. To our knowledge, only one other study has reported linear correlations between thiophene HDS activity and CO and O_2 chemisorption capacities for the same sulfided Mo/Al_2O_3 catalysts (32). The discrepancy between the turnover frequencies calculated from the data of Bachelier *et al.* (see Results) of 0.024 ± 0.001 s^{-1} and 0.0046 ± 0.0002 s^{-1} based upon titration of sites by CO and O_2 chemisorption, respectively, can be traced to the temperature of 333 K at which the O_2 chemisorption measurements were performed. As discussed in the Results section, studies by Massoth and co-workers (17) indicate that O_2 undergoes a slow reaction with sulfided Mo/Al_2O_3 catalysts at

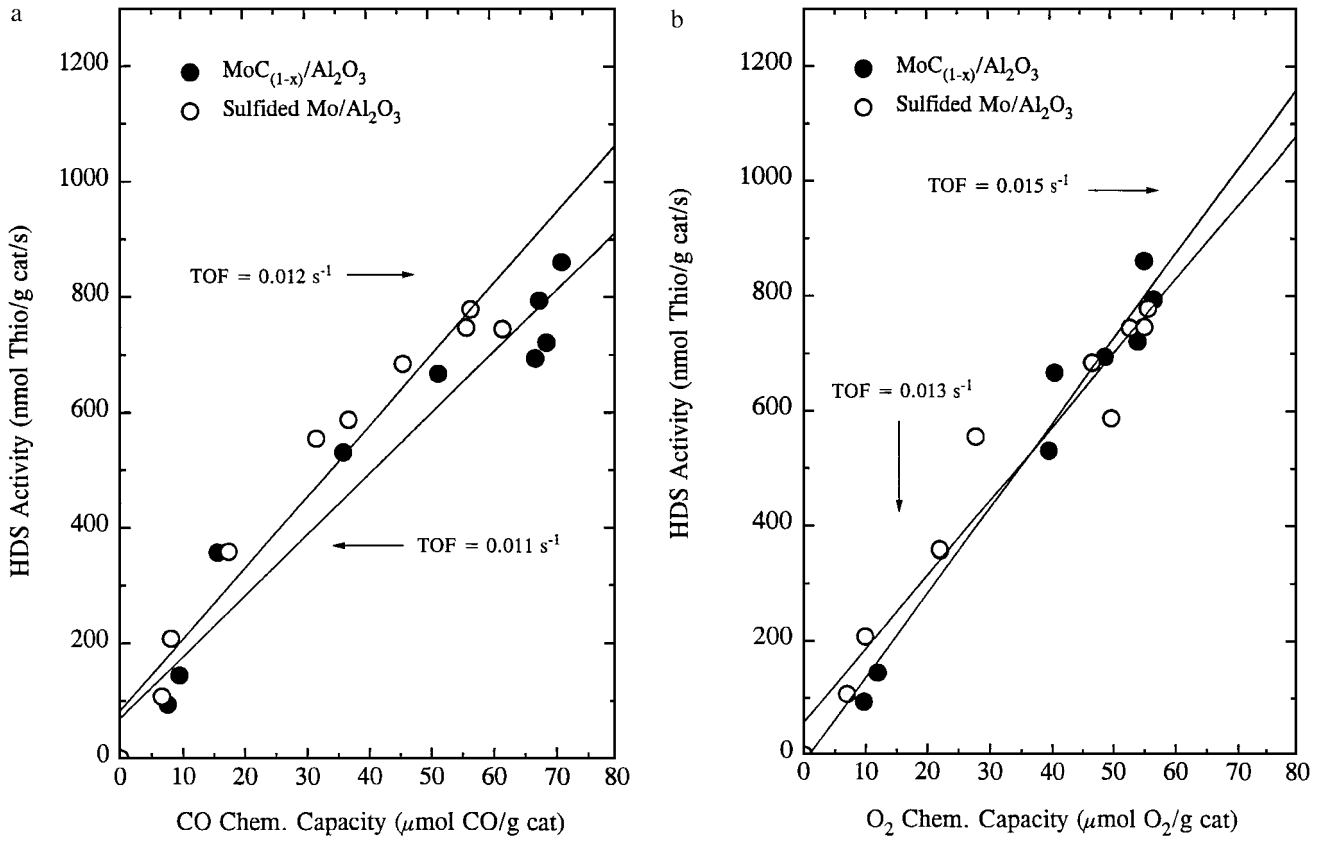

FIG. 10. Correlation of thiophene HDS activity with (a) CO and (b) O_2 chemisorption capacities for $MoC_{(1-x)}/Al_2O_3$ and sulfided Mo/Al_2O_3 catalysts with Mo loadings in the range 1.5–20 wt%.

temperatures of 273 K and above, resulting in an overestimation of the number of adsorption sites on these catalysts. Consequently, the turnover frequency calculated using the HDS activity and O_2 chemisorption data of Bachelier *et al.* is substantially lower than the value determined using their CO chemisorption data (32). The close agreement of the thiophene turnover frequencies calculated using our CO and O_2 chemisorption data suggests that 196 K is an appropriate temperature to carry out O_2 titration of sites on sulfided Mo/Al_2O_3 catalysts.

The data plotted in Figs. 9–11 show that linear correlations between thiophene HDS activity and CO and O_2 chemisorption capacities also hold for Mo_2C/Al_2O_3, $MoC_{(1-x)}/Al_2O_3$, and Mo_2N/Al_2O_3 catalysts. As noted on the figures, the slopes of the linear regressions of the thiophene HDS activity versus chemisorption capacity plots are the turnover frequencies for the Mo carbide, nitride, and sulfided Mo catalysts. The turnover frequencies (± one std. dev.) listed in Table 6 provide further support of our conclusion that the active sites for thiophene HDS are identical on Mo_2C/Al_2O_3, $MoC_{(1-x)}/Al_2O_3$, Mo_2N/Al_2O_3, and sulfided Mo/Al_2O_3 catalysts. The turnover frequencies based upon titration of sites with O_2 are essentially identical while the turnover frequencies based upon titration of sites with CO are also quite similar. These results suggest that the higher HDS activity of Mo_2C/Al_2O_3 and Mo_2N/Al_2O_3 catalysts when compared to sulfided Mo/Al_2O_3 catalysts is associated with a higher density of sites rather than more active sites.

There are at least two possible explanations for the higher site densities on Mo_2C/Al_2O_3, $MoC_{(1-x)}/Al_2O_3$, and Mo_2N/Al_2O_3 catalysts when compared to sulfided Mo/Al_2O_3 catalysts. The first relates to the structures of the different materials. Molybdenum carbides and nitrides are interstitial alloys which can be expected to expose Mo atoms on all crystal faces (14). Molybdenum disulfide (MoS_2), on the other hand, is a layered dichalcogenide material which has a highly anisotropic structure (38). The basal plane of MoS_2 consists of a close-packed layer of sulfur atoms, Mo atoms are exposed only on edge planes. There is good agreement among researchers that the active sites for HDS over sulfided Mo/Al_2O_3 catalysts are coordinately unsaturated (*cus*) Mo^{2+} sites located on the edge planes of MoS_2 crystallites (39). One might expect, therefore, that Mo_2C/Al_2O_3, $MoC_{(1-x)}/Al_2O_3$, and Mo_2N/Al_2O_3 catalysts would have a higher density of active HDS sites than sulfided Mo/Al_2O_3 catalysts. The chemisorption data listed in Tables 1–4 and plotted in Fig. 5 support this

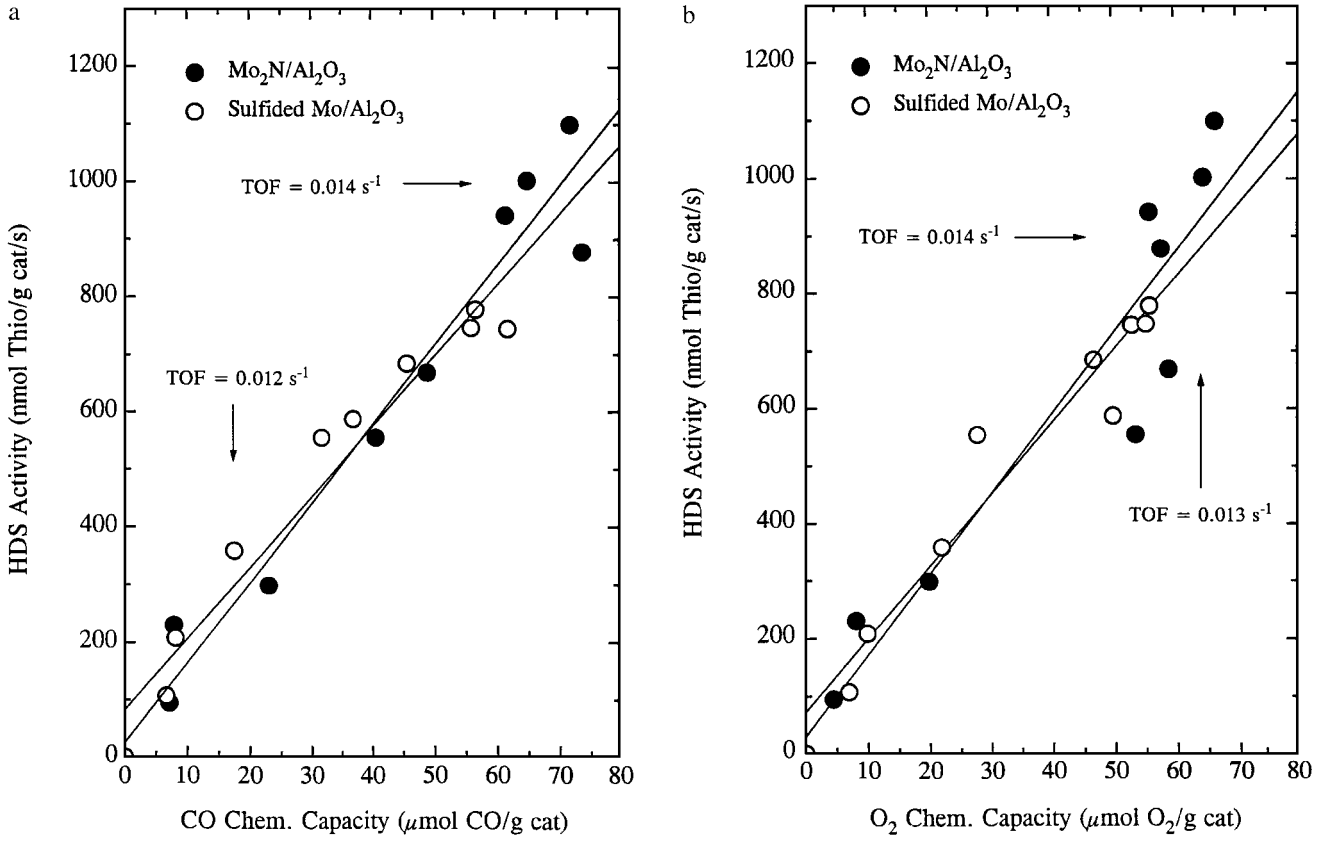

FIG. 11. Correlation of thiophene HDS activity with (a) CO and (b) O_2 chemisorption capacities for Mo_2N/Al_2O_3 and sulfided Mo/Al_2O_3 catalysts with Mo loadings in the range 1.5–20 wt%.

conclusion as the reduced Mo carbide and nitride catalysts have consistently higher CO and O_2 chemisorption capacities than do sulfided Mo/Al_2O_3 catalysts with the same Mo loading.

A second, and we believe more likely, explanation for the higher site densities on Mo carbide and nitride catalysts when compared to sulfided Mo catalysts is based upon a previously proposed model (12) in which alumina-supported β-Mo_2C and γ-Mo_2N particles act as supports for a thin, sulfided Mo layer exposing a high density of active HDS sites (Fig. 1). In the case of Mo_2C/Al_2O_3 and Mo_2N/Al_2O_3 catalysts, the mechanical properties of high hardness and strength, which make transition metal carbides and nitrides desirable for many wear-related applications, along with high melting points may permit β-Mo_2C and γ-Mo_2N particles to serve as rigid substrates for a highly dispersed or strained, sulfided Mo phase. The concept of a strained MoS_2 layer to explain high catalyst activity was recently invoked by Dayte *et al.* (40). These authors carried out pyridine HDN measurements over sulfided Mo/TiO_2 and sulfided $Mo/TiO_2/SiO_2$ catalysts and found the latter catalysts to be considerably more active. Transmission electron microscopy (TEM) showed the sulfided $Mo/TiO_2/SiO_2$ catalysts to consist of silica supported, nanometer-sized TiO_2 protuberances which were covered by single layers of MoS_2 (40). As clearly shown in the TEM micrographs, MoS_2 layers supported on the TiO_2 protuberances are highly curved, giving them a fan-like appearance. The authors suggest that this curvature causes strain in the MoS_2 layer which may create additional sites than are present on "flat" MoS_2 layers.

The similarity in size of the MoS_2 covered titania protuberances (2–5 nm) of the sulfided $Mo/TiO_2/SiO_2$ catalysts of Dayte *et al.* to the alumina-supported Mo carbide and nitride particles (<6 nm for Mo loadings <30 wt%) in our work leads us to suggest that similar MoS_2 layers may be formed on our catalysts. As the chemisorption data listed in Tables 1, 3, and 4, and plotted in Fig. 5 indicate, *sulfided* Mo_2C/Al_2O_3 and Mo_2N/Al_2O_3 catalysts have consistently higher CO and O_2 chemisorption capacities than sulfided Mo/Al_2O_3 catalysts with the same Mo loading. The supported Mo carbide and nitride particles may simply serve as a template on which a strained or highly dispersed, sulfided Mo phase is formed. In this sense, carbon and nitrogen can be considered as textural promoters, acting to increase the number of active sites instead of their activity.

While we believe the model advanced in the previous paragraph provides a good framework for understanding the differences in the thiophene HDS activities of

alumina-supported Mo carbide, nitride, and sulfided Mo catalysts, it does not appear to completely explain the catalytic data reported in this study. Most prominently, it is not obvious how to reconcile with the model the substantially different thiophene HDS activities of the two phases of molybdenum carbide, β-Mo_2C and α-$MoC_{(1-x)}$ ($x \approx 0.5$) (Tables 1, 2, and 5). The O_2 chemisorption capacities of *sulfided* $MoC_{(1-x)}/Al_2O_3$ catalysts adsorb somewhat less O_2 than do *sulfided* Mo_2C/Al_2O_3 catalysts, indicating a lower density of active sites on the $MoC_{(1-x)}$ catalysts. Based upon these results, one might conclude that the morphology of the supported α-$MoC_{(1-x)}$ ($x \approx 0.5$) particles does not allow formation of the strained/highly-dispersed sulfided Mo layer on their surfaces. However, the CO chemisorption capacities for the two supported Mo carbide phases, sulfided prior to chemisorption measurements, are almost the same for the entire range of Mo loadings, suggesting similar active site densities. Additional studies will be necessary to fully understand this dependence of thiophene HDS activity on Mo carbide phase.

CONCLUSIONS

Alumina-supported Mo carbide and nitride catalysts have been prepared and evaluated for use in the hydrodesulfurization process. When normalized per gram of catalyst or mole of molybdenum, Mo_2C/Al_2O_3 and Mo_2N/Al_2O_3 catalysts have significantly higher thiophene HDS activities than conventional sulfided Mo/Al_2O_3 catalysts for Mo loadings in the range 1.5–20 wt%. In contrast, $MoC_{(1-x)}/Al_2O_3$ catalysts were observed to have HDS activities similar to those of sulfided Mo/Al_2O_3 catalysts. When the HDS activities of the different catalysts are normalized using either their CO or O_2 chemisorption capacities, the resulting turnover frequencies are quite similar. These results provide new evidence to support a previously proposed model for the active surface of alumina-supported Mo carbide and nitride catalysts in which a thin layer of sulfided Mo is present on the surface of the Mo carbide and nitride particles. The higher activity of Mo_2C/Al_2O_3 and Mo_2N/Al_2O_3 catalysts is primarily due to a higher density of active sites on this strained/highly-dispersed sulfided Mo layer.

ACKNOWLEDGMENTS

This research was supported by the National Science Foundation under Grant CHE-9400740. Acknowledgment is also made to the Henry Dreyfus Teacher-Scholar Awards Program of the Camille and Henry Dreyfus Foundation for partial support of this research. The authors also acknowledge the efforts of Paul A. Aegerter and Garth J. Simpson in the early stages of this study and Professor David Patrick for helpful discussions.

REFERENCES

1. Schlatter, J. C., Oyama, S. T., Metcalfe, J. E., and Lambert J. M., *Ind. Eng. Chem. Res.* **27**, 1648 (1988).
2. Sajkowski, D. J., and Oyama, S. T., *ACS. Div. Petrol. Prepr.* **35**, 233 (1990).
3. Sajkowski, D. J., and Oyama, S. T., *Appl. Catal. A*, **134**, 339 (1996).
4. Nagai, M., and Miyao, T., *Catal. Lett.* **15**, 105 (1992).
5. Lee, K. S., Abe, H., Reimer, J. A., and Bell, A. T., *J. Catal.* **139**, 34 (1993).
6. Choi, J. G., Brenner, J. R., Colling, C. W., Demczyk, B., Dunning, J. L., and Thompson, L. T., *Catal. Today* **15**, 201 (1992).
7. Abe, H., and Bell, A. T., *Catal. Lett.* **18**, 1 (1993).
8. Colling, C. W., and Thompson, L. T., *J. Catal.* **146**, 193 (1994).
9. Lee, J. S., and Boudart, M., *Appl. Catal.* **19**, 207 (1985).
10. Markel, E. J., and Van Zee, J. W., *J. Catal.* **126**, 643 (1990).
11. Nagai, M., Miyao, T., and Tuboi, T., *Catal. Lett.* **18**, 9 (1993).
12. Aegerter, P. A., Quigley, W. W. C., Simpson, G. J., Ziegler, D. D., Logan, J. W., McCrea, K. R., Glazier, S., and Bussell, M. E., *J. Catal.* **164**, 109 (1996).
13. Park, H. K., Lee, J. K., Yoo, J. K., Ko, E. S., Kim, D. S., and Kim, K. L., *Appl. Catal.* **150**, 21 (1997).
14. Oyama, S. T., *Catal. Today* **15**, 179 (1992).
15. Lee, J. S., Lee, K. H., and Lee, J. Y., *J. Phys. Chem.* **96**, 362 (1992).
16. Tauster, S. J., Pecoraro, T. A., and Chianelli, R. R., *J. Catal.* **63**, 515 (1980).
17. Zmierczak, W., MuraliDhar, G., and Massoth, F. E., *J. Catal.* **77**, 432 (1982).
18. Bachelier, J., Tilliette, M. J., Duchet, J. C., and Cornet, D., *J. Catal.* **76**, 300 (1982).
19. Levy, R. B., *in* "Advanced Materials in Catalysis" (J. J. Burton and R. L. Garten, Eds.), p. 101. Academic Press, San Diego, 1977.
20. Lee, J. S., Yeom, M. H., Park, K. Y., Nam, I. S., Chung, J. S., Kim, Y. G., and Moon, S. H., *J. Catal.* **128**, 126 (1991).
21. Spies, G. H., and Angelici, R. J., *Organometallics* **6**, 1897 (1987).
22. McClune, W. F. (Ed.), Card 35-787, JCPDS Powder Diffraction File (Inorganic), 1992.
23. McClune, W. F. (Ed.), Card 15-457, JCPDS Powder Diffraction File (Inorganic), 1992.
24. McClune, W. F. (Ed.), Card 25-1366, JCPDS Powder Diffraction File (Inorganic), 1992.
25. Diaz, A. L., and Bussell, M. E., *J. Phys. Chem.* **97**, 470 (1993).
26. Lee, J. S., Locatelli, S., Oyama, S. T., and Boudart, M., *J. Catal.* **125**, 157 (1990).
27. Lee, J. S., and Boudart, M., *Catal. Lett.* **20**, 97 (1993).
28. Goldschmidt, H. J., "Interstitial Alloys," p. 360, Plenum, New York, 1967.
29. Lee, J. S., Volpe, L., Ribeiro, F. H., and Boudart, M., *J. Catal.* **112**, 44 (1988).
30. Ranhotra, G. S., Bell, A. T., and Reimer, J. A., *J. Catal.* **108**, 40 (1987).
31. Aegerter, P. A., M.S. thesis, Western Washington University, 1996.
32. Bachelier, J., Duchet, J. C., and Cornet, D., *Bull. Soc. Chim. Belg.* **90**, 1301 (1981).
33. Topsøe, N.-Y., and Topsøe, H., *J. Catal.* **75**, 354 (1982).
34. Topsøe, H., Clausen, B. S., Topsøe, N.-Y., and Pederson, E., *Ind. Eng. Chem. Fund.* **25**, 25 (1986).
35. Okamoto, Y., Maezawa, A., and Imanaka, T., *J. Catal.* **120**, 29 (1989).
36. Miciukiewicz, J., Zmierczak, W., and Massoth, F. E., *Bull. Soc. Chim. Belg.* **96**, 915 (1987).
37. Bodrero, T. A., Bartholomew, C. H., and Pratt, K. C., *J. Catal.* **78**, 253 (1982).
38. Wold, A., and Dwight, K., "Solid State Chemistry: Synthesis, Structure and Properties of Selected Oxides and Sulfides," Chapman & Hall, New York, 1993.
39. Müller, B., van Langeveld, A. D., Moulijn, J. A., and Knözinger, H., *J. Phys. Chem.* **97**, 9028 (1993).
40. Dayte, A. K., Srinivasan, S., Allard, L. F., Peden, C. H. F., Brenner, J. R., and Thompson, L. T., *J. Catal.* **158**, 205 (1996).